EurJIC European Journal of Inorganic Chemistry
ChemPubSoc Europe
FULL PAPER

DOI:10.1002/ejic.201402992

Nitric Oxide and Nitroxyl Products from the Reaction of L-Cysteine with *trans*-$[RuNO(NH_3)_4P(OEt)_3](PF_6)_3$

José Clayston Melo Pereira,[a,b] Maykon Lima Souza,[a] and Douglas Wagner Franco*[a]

Keywords: Nitric oxide / Nitroxyl / Nitrogen oxides / Ruthenium / Kinetics / Medicinal chemistry

The reaction between the *trans*-$[RuNO(NH_3)_4P(OEt)_3](PF_6)_3$ and L-cysteine (RS^-) was studied over a pH range of 2.0–7.4. In this reaction, the concentrations of NO and HNO produced varied as a function of the pH of the solution. The first step of this reaction proceeded quickly [$k_1 = (3.5 \pm 0.3) \times 10^3$ M^{-1} s^{-1}, pH = 3.5, 25 °C] and resulted in the formation of *trans*-$[Ru(NH_3)_4P(OEt)_3N(O)SR]^{2+}$, which dissociated to yield *trans*-$[Ru(NH_3)_4P(OEt)_3NO^{\cdot}]^{2+}$ and $RS^{\cdot}$. However, *trans*-$[Ru(NH_3)_4P(OEt)_3N(O)SR]^{n-1}$ *can* react with a second L-cysteine, yielding *trans*-$[Ru(NH_3)_4P(OEt)_3N(O)(SR)_2]^+$ [$k_2 = (3.6 \pm 0.1)$ M^{-1} s^{-1}, pH = 3.5, 25 °C]. Therefore, the *trans*-$[Ru(NH_3)_4P(OEt)_3NO^{\cdot}]^{2+}$ species released NO and the *trans*-$[Ru(NH_3)_4P(OEt)_3N(O)(SR)_2]^{n-2}$ species released HNO.

Introduction

Nitric oxide (NO) plays fundamental roles in biological processes such as immune responses, blood-pressure control, neurotransmission and carcinogenesis.[1,2] Nitroxyl (HNO), the product of nitric oxide reduction, has been reported to be a more effective vasodilator than NO and to exhibit a protective effect against heart failure. This finding suggests that the HNO donors are a promising new class of vasodilators.[3–7]

The principal targets for NO under bioregulated conditions are metal centers with low oxidation states, primarily iron proteins.[8] In general, HNO interacts preferentially with thiols and ferric hemes, which are intermediates in the catalytic cycles of heme-based nitrite and nitric oxide reductases.[8] Therefore, both NO and HNO molecules exhibit relevant biological functions.[8–10] Focus has been placed on the biological processes of the interactions of these nitric oxide species with a metal center and on their redox interconversions [$M(NO^+)/M(NO)$ or $M(NO^-)/M(HNO)$].[11] This chemical knowledge was obtained through the synthesis and characterization of nitric oxide complexes.[11] For example, the *trans*-$[Ru(NO)(NH_3)_4\{P(III)\}_3]^{3+}$ species [where P(III) = $P(OEt)_3$ or $P(OH)(OEt)_2$] selectively releases NO or HNO electrochemically or through the chemical reduction of the nitrosonium ligand (NO^+).[12,13] The reaction between *trans*-$[RuNO(NH_3)_4\{P(III)\}_3](PF_6)_3$ and europium(II), which is a one-electron reductant, quantitatively yields NO.[12] In addition, the reaction between the *trans*-$[RuNO(NH_3)_4\{P(III)\}_3](PF_6)_3$ complex and Zn(Hg) (a two-electron reductant) quantitatively yields HNO.[12,13] The antileishmanial and antitrypanosomal effects of the following complexes were ascribed to their nitric oxide and nitroxyl release capacities when activated by one or two electron reductions, respectively: *trans*-$[Ru(NO)(NH_3)_4L]X_3$, where X = BF_4^-, PF_6^- or Cl^- and L = imidazole (imN), 4-picoline (4-pic), pyrazine (pz), pyridine (py), triethylphosphite [$P(OEt)_3$], L-histidine (L-hist), isonicotinamide (isn), sulfite (SO_3^{-2}) or nicotinamide (nic), see Equations (1) and (2).[10,12–15]

$$t\text{-}[Ru(NH_3)_4(L)(NO)]^{3+} + 1e^- \xrightarrow{H_2O} t\text{-}[Ru(NH_3)_4(L)(H_2O)]^{2+} + NO \quad (1)$$

$$t\text{-}[Ru(NH_3)_4(L)(NO)]^{3+} + 2e^- \xrightarrow{2H_2O} t\text{-}[Ru(NH_3)_4(L)(H_2O)]^{2+} + HNO + OH^- \quad (2)$$

Thiols are abundant in biological media and their redox potentials are adequate for reactions with the nitrosonium ligand.[16] Thiols are therefore natural candidates for activating nitrosyl complexes in vivo. Indeed, in a related paper,[10] evidence was presented indicating L-cysteine reacts with *trans*-$[Ru(NO)(NH_3)_4P(OEt)_3]^{3+}$ to yield final products of NO and HNO. To gain additional insight into the

[a] Instituto de Química de São Carlos, Universidade de São Paulo,
Av. Trabalhador São Carlense, CEP: 13560-970 – São Carlos – SP, Brazil
E-mail: douglas@iqsc.usp.br
www.iqsc.usp.br
[b] Departamento de Química Geral e Inorgânica, Instituto de Química de Araraquara, UNESP – Universidade Estadual Paulista,
P. O. Box 355, Araraquara, São Paulo 14801-970, Brazil
Supporting information for this article is available on the WWW under http://dx.doi.org/10.1002/ejic.201402992.

chemical reactivity of nitrosyl complexes with thiols, we here investigated the reaction between *trans*-$[Ru(NO)(NH_3)_4P(OEt)_3]^{3+}$ and L-cysteine.

Results and Discussion

As previously reported,[17–20] the reactions between nitrosyl ruthenium complexes and nucleophilic agents, such as cysteine and glutathione, occur according to the reaction sequences shown in Equations (3) and (4).

$$[Ru(L)_5NO]^n + RS^- \rightleftharpoons [Ru(L)_5N(O)SR]^{n-1} \quad (3)$$

$$[Ru(L)_5N(O)SR]^{n-1} + RS^- \rightleftharpoons [Ru(L)_5N(O)(SR)_2]^{n-2} \quad (4)$$

Here, $[Ru(L)_5N(O)SR]^{n-1}$ is produced through interactions between the thiol and the nitrosonium ligand. The interactions of a second thiol molecule with $[Ru(L)_5N(O)SR]^{n-1}$ may result in the formation of $[Ru(L)_5N(O)(SR)_2]^{n-2}$ [Equation (3) and Equation (4)].

The production of the aqua ruthenium complex, cystine (RSSR), and N_2O[18] or NO[20] occurs in the sequences depicted in Equations (5) and (6).

$$[Ru(L)_5N(O)(SR)_2]^{n-2} \xrightarrow{H_2O} [Ru(L)_5(H_2O)]^{n-1} + 1/2N_2O + RSSR \quad (5)$$

$$[Ru(L)_5N(O)(SR)_2]^{n-2} \xrightarrow{H_2O} [Ru(L)_5(H_2O)]^{n-1} + NO + 1/2RSSR + RS^- \quad (6)$$

Therefore, the reaction between the *trans*-$[Ru(NH_3)_4P(OEt)_3NO]^{3+}$ complex and cysteine would likely follow a pathway similar to those previously mentioned[18–20] [Equation (5) and Equation (6)]. To verify these hypotheses, we conducted kinetic studies and product analyses for these reactions.

Production of NO and HNO from the Reaction between the Nitrosyl Complex and L-Cysteine

The reaction was monitored by using infrared spectroscopy and chronoamperometry. After mixing aqueous solutions of the complex *trans*-$[Ru(NH_3)_4P(OEt)_3NO]^{3+}$ (**1**) and L-cysteine, we detected free nitric oxide as indicated by an increase in the IR absorbance at 1872 cm^{-1} ($\tilde{\nu}_{NO}$ in $RuNO^0$) with a simultaneous decrease in the absorbance at 1923 cm^{-1}, which corresponds to the $\tilde{\nu}_{NO^+}$ in $RuNO^+$[17] (Figure 1).

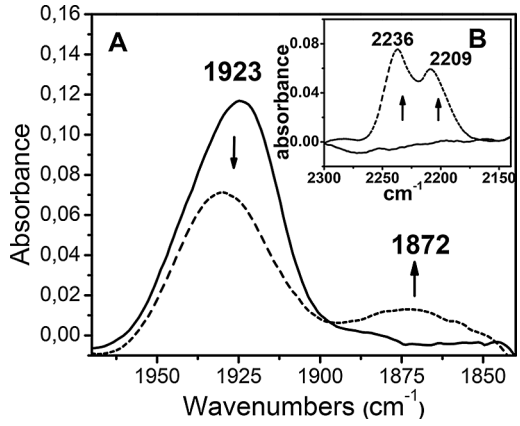

Figure 1. Vibrational spectrum of the mixture of *trans*-$[RuNO(NH_3)_4P(OEt)_3](PF_6)_3$ and L-cysteine. Insert: peaks ascribed to N_2O. Conditions: [Ru] = 1×10^{-1} mol L^{-1}, $[cys]_{tot}$ = 1.2×10^{-1} mol L^{-1}, pH 4.5, μ = 0.2 mol L^{-1}.

The IR spectrum of the solution containing *trans*-$[Ru(NO)(NH_3)_4P(OEt)_3]^{3+}$ and cysteine displayed absorbance increases at 2236 and 2209 cm^{-1}, which were attributed to the presence of N_2O.[19,21] Because N_2O can be a product of HNO dimerization ($k_d = 8.0 \times 10^6$ $M^{-1}s^{-1}$) and because of the high concentration of the reagents, this observation strongly suggests that nitroxyl could be formed from this reaction.[12,21]

According to the chronoamperometric data, which were corroborated by nitric oxide analyzer (NOA) measurements (Figure S1, Supporting Information), the formation of NO from the above reactions is pH dependent (Figure 2). The concentration of liberated NO increased when the pH was increased from 2.0 to 4.0 and decreased when the pH was increased beyond 4.0.

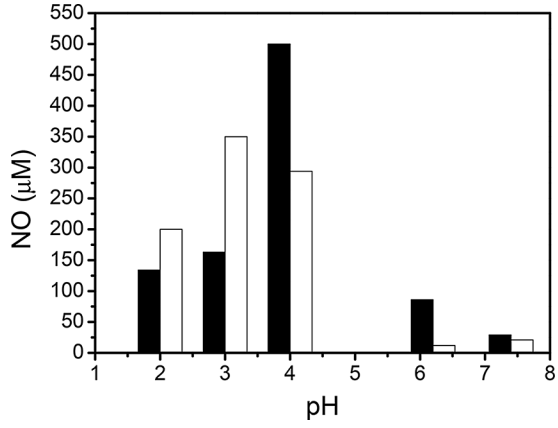

Figure 2. Nitric oxide formation in the reaction between *trans*-$[Ru(NH_3)_4P(OEt)_3NO]^{3+}$and L-cysteine (at two different concentrations) as a function of the solution pH. Experimental conditions: [Ru] = 5×10^{-4} mol L^{-1}, ■ $[cys]_{tot}$ = 5×10^{-3} mol L^{-1}, □ $[cys]_{tot}$ = 5×10^{-2} mol L^{-1}; $[cys]_{tot}$ = ($[RS^-]$ + [RSH]), T = 25 °C.

Assuming that the reaction between cysteine and the nitrosyl complex involves a one-electron reduction of the *trans*-$[Ru(NH_3)_4P(OEt)_3NO]^{3+}$ species, only 6% of the total NO expected to form was observed at pH 7.4. In contrast,

when $Na_3[Fe(CN)_6]$ was simultaneously added to the solution (pH 7.4) with the *trans*-$[RuNO(NH_3)_4P(OEt)_3](PF_6)_3$, the amount of NO formed reached 36% of the expected value.[10] This increase in the NO concentration is consistent with the presence of HNO in the medium, which likely reacted with $[Fe(CN)_6]^{3-}$ to generate the additional nitric oxide[22] through the following reaction [Equation (7)].

$$[Fe^{III}(CN)_6]^{3-} + HNO \rightleftharpoons [Fe^{II}(CN)_6]^{4-} + NO + H^+ \quad (7)$$

In addition, Figure 2 illustrates the effect on the production of NO by this system upon increasing the L-cysteine concentration. Notably, as the $[RS]_{tot}$ was increased from 5×10^{-3} to 5×10^{-2} M in the presence of the ruthenium complex (5×10^{-4} M), the amount of NO produced increased in the pH range of 2.0–4.0 reaching a maximum value at pH 4.0 and which significantly decreased at pH values higher than 4.0. Given that the pK_a of cysteine is 8.3,[23] this behavior is consistent with an increase in the concentration of deprotonated L-cysteine, which inhibits NO production.

Formation of *trans*-$[Ru(NH_3)_4P(OEt)_3N(O)SR]^{2+}$ Species

The reaction of L-cysteine with *trans*-$[Ru(NH_3)_4P(OEt)_3NO]^{3+}$ was monitored on the basis of the changes in the electronic spectra using stopped-flow and conventional techniques (Figure 3, A and B). The initial spectrum of the solution underwent a change in the millisecond timescale upon reaction of *trans*-$[Ru(NH_3)_4P(OEt)_3NO]^{3+}$ with cysteine. An increase in the absorbances at 316 and 465 nm was noticed (Figure 3, B) with respect to the starting solution.

On the basis of the experimental data and information reported in the literature[17–20,22] for related systems, a nucleophilic attack on the nitrogen by a thiol sulfur atom, such as in the reactions illustrated in Equations (8) and (9) is anticipated.

$$t\text{-}[Ru(NH_3)_4P(OEt)_3NO]^{3+} + RSH \underset{k_{-1(RSH)}}{\overset{k_{1(RSH)}}{\rightleftharpoons}} t\text{-}[Ru(NH_3)_4P(OEt)_3N(O)SR]^{2+} + H^+ \quad (8)$$

$$t\text{-}[Ru(NH_3)_4P(OEt)_3NO]^{3+} + RS^- \underset{k_{-1(RS^-)}}{\overset{k_{1(RS^-)}}{\rightleftharpoons}} t\text{-}[Ru(NH_3)_4P(OEt)_3N(O)SR]^{2+} \quad (9)$$

On the basis of the changes in absorbance (Figure 3, A), the assumption that $[RS]_{tot} = [RS^-] + [RSH]$ and the expression in Equation (10)

$$k_{obs} = k_1 + k_{-1}[RS]_{tot} \quad (10)$$

we calculated a rate constant of $k_{1(RS)tot} = (3.5 \pm 0.3) \times 10^3\ mol^{-1}\,L\,s^{-1}$ and $k_{-1(RS)tot} = (4.7 \pm 0.5) \times 10^1\ s^{-1}$ at pH 3.5 (Figure S2, Supporing Information).

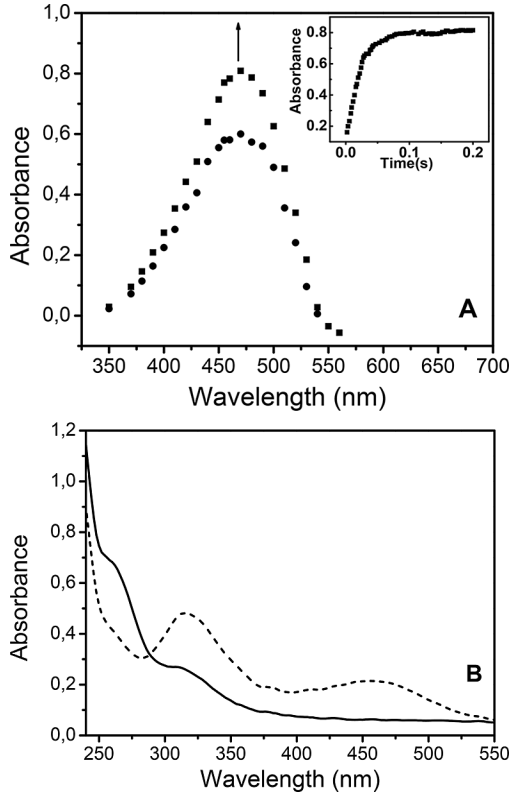

Figure 3. (A) spectroscopic change for the reaction solution of *trans*-$[Ru(NH_3)_4P(OEt)_3NO]^{3+}$ and cysteine monitored by the stopped-flow technique. Insert: absorbance as a function of the time (s) for the reaction monitored using the stopped-flow technique. (B) Electronic spectra of *trans*-$[Ru(NH_3)_4P(OEt)_3NO]^{3+}$ (—) and of the products of the reaction between *trans*-$[Ru(NH_3)_4P(OEt)_3NO]^{3+}$ and L-cysteine (---). Experimental conditions: [Ru] = 5×10^{-4} mol L^{-1}, $[cys]_{tot} = 5 \times 10^{-3}$ mol L^{-1}, pH = 3.5, μ = 0.2 mol L^{-1}, T = 25 °C.

Formation of *trans*-$[Ru(NH_3)_4P(OEt)_3N(O)(SR)_2]^+$ Species

The formation of *trans*-$[Ru(NH_3)_4P(OEt)_3N(O)(SR)_2]^+$ occurs in the slower second step (Table 1) of the reaction in a matter of seconds, resulting in an absorbance decrease at

Table 1. Kinetic results for the reaction between L-cysteine and *trans*-$[Ru(NH_3)_4P(OEt)_3NO]^{3+}$.

Step 1	k_1 [M^{-1} s^{-1}]	Step 2	k_2 [M^{-1} s^{-1}]
$(RS)_{total}$[a]	3.5×10^3	$(RS)_{total}$[a]	3.6
(RS^-)	1.4×10^8	(RS^-)	1.6×10^4

[a] pH 3.5 (0.1 mM, acetate buffer), T = 25 °C, $[RS]_{tot} = [RS^-] + [RSH]$.

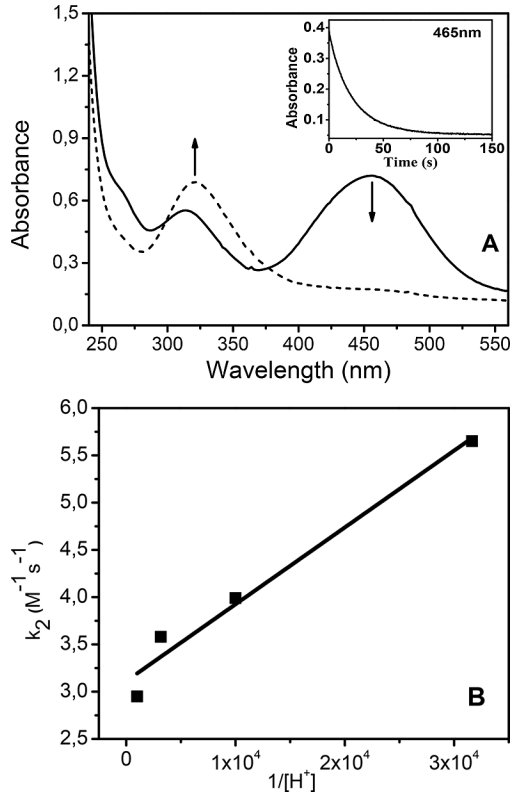

Figure 4. (A) Electronic spectra of *trans*-$[Ru(NH_3)_4P(OEt)_3N(O)SR]^{2+}$ (—) and *trans*-$[Ru(NH_3)_4P(OEt)_3N(O)SR_2]^{+}$ (---). Insert: absorbance vs. time (s). Experimental conditions: [Ru] = 5×10^{-4} mol L^{-1}, $[cys]_{tot}$ = 5×10^{-3} mol L^{-1}, pH = 4.5, μ = 0.2 mol L^{-1}, T = 25 °C. (B) Values of k_2 vs. pH for the reaction of *trans*-$[Ru(NH_3)_4P(OEt)_3NO]^{3+}$ and L-cysteine. μ = 0.2 mol L^{-1}, T = 25 °C.

465 nm and a simultaneous increase in the solution absorbance at 320 nm (Figure 4, A).

The k_2 values calculated from these spectroscopic changes (Figure 4, B) were pH dependent, as show in Equations (11) and (12) and were calculated as $k_{2(RS)tot}$ = (3.6 ± 0.1) M^{-1} s^{-1} and $k_{-2(RS)tot}$ = $(3.8\pm0.8)\times10^{-3}$ s^{-1} at pH 3.5 (Figure S3, Supporting Information) when considering the total $[RS]_{tot}$ = ($[RS^-]$ + [RSH]).

$$t\text{-}[Ru(NH_3)_4P(OEt)_3N(O)SR]^{2+} + RSH \underset{k_{-2(RSH)}}{\overset{k_{2(RSH)}}{\rightleftharpoons}} t\text{-}[Ru(NH_3)_4P(OEt)_3N(O)(SR)_2]^{+} + H^+ \quad (11)$$

$$t\text{-}[Ru(NH_3)_4P(OEt)_3N(O)SR]^{3+} + RS^- \underset{k_{-2(RS^-)}}{\overset{k_{2(RS^-)}}{\rightleftharpoons}} t\text{-}[Ru(NH_3)_4P(OEt)_3N(O)(SR)_2]^{2+} \quad (12)$$

According to the literature,[18] this step of the reaction between nitrosyl ruthenium complexes and a thiol can be expressed as shown in Equations (13) and (14).

$$k_2 = \frac{k_{2(RS^-)}K_a + k_{2(RSH)}[H^+]}{K_a + [H^+]} \quad (13)$$

$$k_{-2} = k_{-2(RS^-)} + k_{-2(RSH)}[H^+] \quad (14)$$

When a pK_a of 8.3 is considered for the reaction of RSH $\rightleftharpoons$ RS^- + H^+ and when $[H^+] >> K_a$, a plot of the second-order rate constant k_2 against 1/[H] should be linear, with the slope and intercept equal to $k_{2(RS^-)}\cdot K_a$ and $k_{2(RSH)}$, respectively (Figure 4, B), as suggested by Rocaroli.[18] Thus, the rate constant $k_{2(RS-)}$ was calculated as $(1.6\pm0.2)\times10^4$ M^{-1} s^{-1} and the intercept was $k_{-2(RS^-)}$ = (3.1 ± 0.2) s^{-1}.

By extrapolating the data from Equation (13) for the first step of the reaction, we calculated k_1 values at pH 3.0 and 3.5 as approximately 1.14×10^8 and 1.76×10^8 M^{-1} s^{-1}, respectively. Thus the estimated average k_1 would be approximately $(1.4\pm0.3)\times10^8$ M^{-1} s^{-1}, which indicates that the first reaction step was much faster than the second reaction step (Table 1).

Degradation of *trans*-$[Ru(NH_3)_4P(OEt)_3N(O)SR]^{n}$ and *trans*-$[Ru(NH_3)_4P(OEt)_3N(O)(SR)_2]^{n-2}$ Species

With time, an additional decrease was observed in the absorbance at 320 nm (on a minute timescale) as the maximum simultaneously shifted to 316 nm (Figure 5). The final solution spectrum corresponds to the *trans*-$[Ru(NH_3)_4P(OEt)_3H_2O]^{2+}$ ion.[24] On the basis of these last spectroscopic changes, a value of k_{obs} = 4.9×10^{-4} s^{-1} was calculated. At first glance, we associated the spectroscopic change with degradation of *trans*-$[Ru(NH_3)_4P(OEt)_3N(O)(SR)]^{2+}$ – see Equations (15) and (16) – or *trans*-$[Ru(NH_3)_4P(OEt)_3N(O)(SR)_2]^{+}$.

$$t\text{-}[Ru(NH_3)_4P(OEt)_3N(O)(SR)]^{2+} + H_2O \xrightarrow{k_3} t\text{-}[Ru(NH_3)_4P(OEt)_3(H_2O)]^{2+} + NO + 1/2RSSR \quad (15)$$

$$t\text{-}[Ru(NH_3)_4P(OEt)_3N(O)(SR)_2]^{+} + 2H_2O \xrightarrow{k_4} t\text{-}[Ru(NH_3)_4P(OEt)_3(H_2O)]^{2+} + HNO + RSSR + OH^- \quad (16)$$

The NO production increased as the *trans*-$[Ru(NH_3)_4P(OEt)_3N(O)SR]^{2+}$ concentration increased until it reached a maximum at pH 4.0 and $[Cys]_{tot}$ = 5×10^{-3} mol L^{-1} (Figure 2). Thus, under these experimental conditions, most of the *trans*-$[Ru(NH_3)_4P(OEt)_3N(O)SR]^{2+}$ ion would generate the *trans*-$[Ru(NH_3)_4P(OEt)_3H_2O]^{2+}$, NO and RS$^{\cdot}$; see Equation (15). Indeed, the *trans*-$[Ru(NH_3)_4P(OEt)_3H_2O]^{2+}$ ion was identified by using UV/Vis spectroscopy (Figure 4, B) and ^{31}P NMR spectroscopy (δ = 148 ppm, Figure S4,

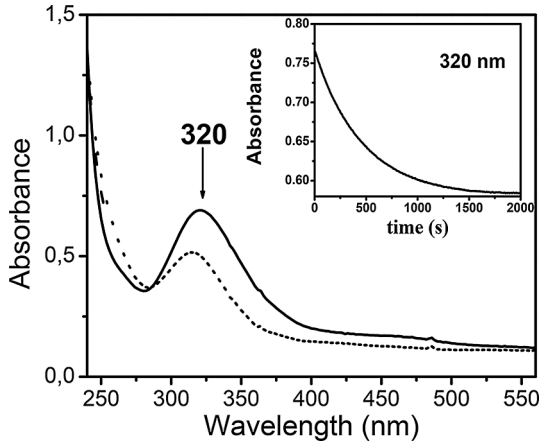

Figure 5. Electronic spectra of the *trans*-$[Ru(NH_3)_4P(OEt)_3N(O)SR]^{3+}$ and *trans*-$[Ru(NH_3)_4P(OEt)_3N(O)SR_2]^{2+}$ decomposition. Insert: absorbance vs. time(s). Experimental conditions: [Ru] = 5×10^{-4} mol L^{-1}, $[cys]_{tot}$ = 5×10^{-3} mol L^{-1}, pH = 4.5, μ = 0.2 mol L^{-1}, T = 25 °C.

Supporting Information).[24] However, in a large concentration of cysteine or at pH greater than 4.0, the concentration of RS^- increases and the NO production decreases because of the likely formation of the *trans*-$[Ru(NH_3)_4P(OEt)_3N(O)(SR)_2]^+$ ion according to Equation (11) and Equation (12). This species is suggested to lead the reduction of the NO^+ ligand by two electrons producing HNO as shown in Equation (16). Thus, under these conditions, production of HNO molecules can be favored. Indeed, HNO has been detected indirectly through the presence of N_2O ($\tilde{\nu}_{N_2O}$ = 2236 and 2209 cm^{-1}) and by the oxidation of HNO to NO during the reaction with $[Fe(CN)_6]^{3-}$ [Equation (7)].[10] Additional support for HNO production in the reaction between *trans*-$[Ru(NO)(NH_3)_4P(OEt)_3]^{3+}$ and cysteine was provided in the literature where metmyoglobin was reported as the nitroxyl scavenger at pH 7.4.[10,25] Therefore, both NO and HNO can be produced from the reaction between *trans*-$[Ru(NO)(NH_3)_4P(OEt)_3]^{3+}$ and cysteine owing to the formation of *trans*-$[Ru(NH_3)_4P(OEt)_3N(O)SR]^{2+}$ [Equation (15)] and *trans*-$[Ru(NH_3)_4P(OEt)_3N(O)(SR)_2]^+$ [Equation (16)], respectively, which occurs as a function of the concentration of RS^-. The aqua complex *trans*-$[Ru(NH_3)_4P(OEt)_3(H_2O)]^{2+}$ is the ruthenium based product formed following the NO and HNO release. The pseudo-first-order rate constant (k_{obs}) for the formation of this aqua complex can be expressed as shown in Equation (17), which shows dependence on the *trans*-$[Ru(NH_3)_4P(OEt)_3N(O)SR]^{2+}$ and *trans*-$[Ru(NH_3)_4P(OEt)_3N(O)(SR)_2]^+$ concentrations.

$$\frac{d[Ru(H_2O)]}{dt} = k_3[RuN(O)SR] + k_4[RuN(O)SR)_2] \quad (17)$$

As has been suggested, the increased formation of the *trans*-$[Ru(NH_3)_4P(OEt)_3N(O)(SR)_2]^+$ ion was associated with decreased NO production. This was identified by conducting the reaction at the same pH and $[RS^-]/[RSH]$ ratio but with increasing cysteine concentrations (Figure 2). This behavior is consistent with the equilibrium constants as shown below in Equations (18), (19), (20) and (21).

$$K_1 = \frac{[RuN(O)SR]\cdot[H^+]}{[RuNO]\cdot RSH]} \quad (18)$$

$$[RuN(O)SR] = K_1[RuNO][RSH][H^+]^{-1} \quad (19)$$

$$K_2 = \frac{[RuN(O)(SR)_2]\cdot[H^+]}{[RuN(O)SR]\cdot RSH]} \quad (20)$$

$$[RuN(O)(SR)_2] = K_1K_2[RuNO]\cdot[RSH]^2[H^+]^{-2} \quad (21)$$

According to Equation (19) and Equation (21), an increase in the solution pH would favor the formation of the *trans*-$[Ru(NH_3)_4P(OEt)_3N(O)(SR)_2]^+$ species over the *trans*-$[Ru(NH_3)_4P(OEt)_3N(O)SR]^{2+}$ species. Therefore, high pH would induce high HNO production.

trans Effect and *trans* Influence of $P(OEt)_3$

Because of the *trans* effect and *trans* influence of the $P(OEt)_3$ ligand,[24] the dissociation of NO from the *trans*-$[Ru(NH_3)_4P(OEt)_3N(O)]^+$ species (in which the Ru^{II}–NO backbonding is very weak)[26] may be faster than in the ruthenium nitrosyl complexes $[Ru(L)_5MNO]^n$ (L = polypyridines, NH_3, EDTA, pz and py).[18] The relatively slow dissociation of NO from other ruthenium ammines i.e. *trans*-$[RuNO(NH_3)_4(L)]^{3+}$, such as L = pyrazine [k_{NO} = 0.07 s^{-1}, $E^0_{(NO^+/NO^0)}$ = 0.112 V vs. NHE][26,27] could facilitate the second nucleophilic attack – see Equations (11) and (12) – resulting in the formation of HNO and reducing the amount of NO formed. Furthermore because the $E^{0'}$ $[RuNO]^{3+}/[RuNO]^{2+}$ in the *trans*-$[Ru(NH_3)_4P(OEt)_3NO]^{3+}$ complex is more positive (+0.132 V vs. NHE)[24] than that in the other tetraammines, the nitrosyl ligand in this compound would be sufficiently active to undergo nucleophilic attack by cysteine even at pH < 3. Scheme 1 illustrates a

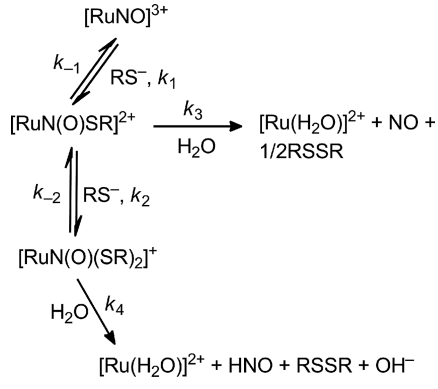

Scheme 1. Reaction between *trans*-$[Ru(NH_3)_4P(OEt)_3NO]^{3+}$ and L-cysteine.

potential mechanism for the reaction between *trans*-$[Ru(NH_3)_4P(OEt)_3NO]^{3+}$ and L-cysteine.

Conclusions

Evidence for the formation of both HNO and NO species was collected for the reaction between L-cysteine and the *trans*-$[Ru(NH_3)_4P(OEt)_3NO]^{3+}$ ion. In addition, the product distribution was found to depend on the RSH/RS^- ratio in solution.

The release of HNO was favored when the *trans*-$[Ru(NH_3)_4P(OEt)_3NO]^{3+}$ complex reacted with L-cysteine at pH 7.4. In this case, the RS^- concentration was perceptible. In macrophage and tumor cells and under metabolic conditions such as hypoxia, where the pH is slightly acidic in relation to normal cells,[28,29] compounds like *trans*-$[Ru(NH_3)_4P(OEt)_3NO]^{3+}$ would work as sources of NO.

Experimental Section

Chemicals and Reagents: All chemicals (unless otherwise indicated) were analytical grade and purchased from Aldrich, Strem or Sigma. Ruthenium trichloride hydrate was the starting material for the synthesis of all of the ruthenium complexes described herein. All solvents were purified following known procedures.[30] Doubly distilled water was used throughout the experiments.

Synthesis of the Complexes: All syntheses and manipulations were conducted under an argon-containing atmosphere.[31] The$[Ru(NH_3)_5Cl]Cl_2$ and *trans*-$[Ru(NO)(NH_3)_4P(OEt)_3](PF_6)_3$ compounds were prepared and characterized as described in the literature.[24,32]

Instruments: UV/Vis measurements were performed in a 1.0 cm quartz cell on a Hitachi U3501 spectrophotometer. For the fast kinetics experiments, an Aminco–Morrow stopped-flow spectrophotometer was used. The temperature was controlled within ±0.1 °C by using a Tecnal TE 184 thermostat. IR spectra were recorded on a Bomem model MB-102 FTIR spectrophotometer from 400 to 4000 cm^{-1} using KBr pellets or in aqueous solutions (CaF_2 windows). The ^{31}P nuclear magnetic resonance (NMR) spectrum was measured in D_2O solution at pH 4.0 (acetate buffer) with NH_4PF_6 as the internal standard and a Bruker AC-200 spectrophotometer.

Measurements: The inert gas (argon or nitrogen with high purity, 99.99%) was deoxygenated (Cr^{II}) prior to use.[18] The complexes were stored under vacuum, protected from light and moisture, and used within a 30-day period. The manipulations of air-sensitive complexes were performed under an argon atmosphere. Next, the solutions were quickly transferred through teflon tubing to a specific tube or cell. Kinetics were investigated by following the absorbance changes at selected wavelengths. All kinetic experiments were conducted under pseudo-first-order conditions with an excess of L-cysteine ($[RS]_{tot} = [RS^-]+[RSH]$) and a metal concentration of 5.0×10^{-4} M at pH values of 3.0–4.5 (25 °C). The pH values of the solutions during the kinetics experiments were maintained below 4.5 to avoid nucleophilic attack of NO^+ and $P(OEt)_3$ ligands by hydroxy ions.[21,24] Furthermore, at pH values greater than 5, the reaction with L-cysteine became too fast for measurement with our equipment. At a pH of 2.0, the sulfur group on the L-cysteine molecule was fully protonated (pK_a = 8.3). In addition, CH_3COOH/CH_3COONa or $C_3H_5O(COOH)_3$/$C_3H_5O(COO)_3Na_3$ were used as buffer solutions and the ionic strength was held constant by using $NaCF_3COO$ as a supporting electrolyte. The observed pseudo-first-order constants ($_{obs}$)were determined from plots of $\ln(A_\infty - A_t)$ vs. time. Following treatment of the data according to $k_{obs} = k_1[L] + k_{-1}$, where L = RSH or RS^-, the specific second-order rate constants were calculated according to the equilibrium equations for the respective reactions. The amount of NO that was released in these solutions was measured by using a selective NO electrode (amino) from Innovative Instruments, Inc. The temperature was maintained at T = 25.0 ± 0.1 °C. The experimental conditions were held constant except for the concentration of L-cysteine, which was varied from 10 to 100 times greater than the concentration of the nitrosyl complex. The *trans*-$[Ru(NO)(NH_3)_4P(OEt)_3](PF_6)_3$ compound (4.0 mg, 500 μM) was dissolved in 10 mL of an Ar-saturated solution containing L-cysteine. The experiments were performed over a pH range of 2.0 to 7.4 at 25 °C. The model 280i nitric oxide analyzer (NOA) from the GE Sievers was also used in the NO measurements at pH 4.0 and 7.4.[33]

Acknowledgments

The authors acknowledge the Brazilian agencies Fundação de Amparo à Pesquisa do Estado de São Paulo (FAPESP), Coordenação de Aperfeiçoamento de Pessoal de Nível Superior (CAPES) and Conselho Nacional de Desenvolvimento Científico e Tecnológico (CNPq) for their financial support. The authors also thank José C. Toledo Jr. (FFCLRP-USP) for NOA measurements.

[1] J. L. E. Ignarro, *Nitric Oxide, Biology and Pathobiology*, Academic Press, San Diego, CA, **2000**.
[2] M. Feelisch, J. S. Stamler (Eds.), *Methods in Nitric Oxide Research*, John Wiley & Sons, New York, **1996**.
[3] H. N. Sabbah, C. G. Tocchetti, M. Wang, S. Daya, R. C. Gupta, R. S. Tunin, R. Mazhari, E. Takimoto, N. Paolocci, D. Cowart, W. S. Colucci, D. A. Kass, *Circ. Heart Fail.* **2013**, *6*, 1250–1258.
[4] N. Paolocci, M. I. Jackson, B. E. Lopez, K. Miranda, C. G. Tocchetti, D. A. Wink, A. J. Hobbs, J. M. Fukuto, *Pharmacol. Ther.* **2007**, *113*, 442–458.
[5] K. M. Miranda, *Coord. Chem. Rev.* **2005**, *249*, 433–455.
[6] J. M. Fukuto, A. J. Hobbs, L. J. Ignarro, *Biochem. Biophys. Res. Commun.* **1993**, *196*, 707.
[7] D. Bonaventura, R. G. de Lima, J. A. Vercesi, R. S. da Silva, L. M. Bendhack, *Vascular Pharmacology* **2007**, *46*, 215.
[8] K. M. Miranda, R. W. Nims, D. D. Thomas, M. G. Espey, D. Citrin, M. D. Bartberger, N. Paolocci, J. M. Fukuto, M. Feelisch, D. A. Wink, *J. Inorg. Biochem.* **2003**, *93*, 52–60.
[9] J. M. Fukuto, C. J. Cisneros, R. L. Kinkade, *J. Inorg. Biochem.* **2013**, *118*, 201–208.
[10] J. C. M. Pereira, V. Carregaro, D. L. Costa, J. S. Silva, F. Q. Cunha, D. W. Franco, *Eur. J. Med. Chem.* **2010**, *45*, 4180.
[11] A. C. Montenegro, V. T. Amorebieta, L. D. Slep, D. F. Martin, F. Roncaroli, D. H. Murgida, S. E. Bari, J. A. Olabe, *Angew. Chem. Int. Ed.* **2009**, *48*, 4213–4216; *Angew. Chem.* **2009**, *121*, 4277.
[12] G. Metzker, E. V. Stefaneli, J. C. M. Pereira, F. C. A. Lima, S. C. da Silva, D. W. Franco, *Inorg. Chim. Acta* **2013**, *394*, 765–769.
[13] D. R. Truzzi, D. W. Franco, *Inorg. Chim. Acta* **2014**, *421*, 74–79.
[14] J. J. N. Silva, W. R. Pavanelli, J. C. M. Pereira, J. S. Silva, D. W. Franco, *Antimicrob. Agents Chemother.* **2009**, *53*, 4414–4421.
[15] E. Tfouni, F. G. Doro, L. E. Figueiredo, J. C. M. Pereira, G. Metzker, D. W. Franco, *Curr. Med. Chem.* **2010**, *17*, 3643–3657.

[16] C. Hwang, A. J. Sinskey, H. F. Lodish, *Science* **1992**, *257*, 1496–1502.
[17] G. Metzker, J. C. Toledo Jr., F. C. A. Lima, A. Magalhães, D. R. Cardoso, D. W. Franco, *J. Braz. Chem. Soc.* **2010**, *21*, 1266–1273.
[18] F. Roncaroli, J. A. Olabe, *Inorg. Chem.* **2005**, *44*, 4719–4727.
[19] F. Roncaroli, M. Videla, L. D. Slep, J. A. Olabe, *Coord. Chem. Rev.* **2007**, *251*, 1903–1930.
[20] F. O. N. Silva, M. C. L. Cândido, A. K. M. Holanda, I. C. N. Diógenes, E. H. S. Sousa, L. G. F. Lopes, *J. Inorg. Biochem.* **2011**, *105*, 624–629.
[21] J. Marhenke, C. A. Joseph, M. Z. Corliss, T. J. Dunn, P. C. Ford, *Polyhedron* **2007**, *26*, 4638–4644.
[22] D. A. Wink, M. Feelisch, J. Fukuto, D. Chistodoulou, D. Jourd'heuil, M. B. Grisham, Y. Vodovotz, J. A. Cook, M. Krishna, W. G. DeGraff, S. Kim, J. Gamson, J. B. Mitchell, *Arch. Biochem. Biophys.* **1998**, *351*, 66–74.
[23] H. P. R. Frederikse, D. R. Lide (Eds.), *CRC Handbook of Chemistry & Physics*, 75th ed., CRC Press, Boca Raton, FL, USA, **1994**.
[24] L. G. F. Lopes, E. E. Castellano, A. G. Ferreira, C. U. Davanzo, M. J. Clarke, D. W. Franco, *Inorg. Chim. Acta* **2005**, *359*, 2883–2890.
[25] D. R. Arnelle, J. S. Stamler, *Arch. Biochem. Biophys.* **1995**, *318*, 279–289.
[26] J. C. Toledo, H. A. S. Silva, M. Scarpellini, V. Mori, A. J. Camargo, M. Bertotti, D. W. Franco, *Eur. J. Inorg. Chem.* **2004**, 1879–1885.
[27] E. Tfouni, M. Krieger, B. McGarvey, D. W. Franco, *Coord. Chem. Rev.* **2003**, *236*, 57–69.
[28] D. Miklavcic, G. Sersa, S. Novakovic, *J. Bioelect.* **1990**, *9*, 133.
[29] J. O. Lundberg, E. Weitzberg, M. T. Gladwin, *Nat. Rev. Drug Discov.* **2008**, *7*, 156–167.
[30] D. D. Perrin, W. L. F. Armarego, D. R. Perrin, *Purification of Laboratory Chemicals*, Pergamon Press, Elmsford, **1980**.
[31] D. F. Shriver, *The Manipulation of Air-Sensitive Compounds*, McGraw-Hill, New York, **1969**.
[32] L. H. Vogt, J. L. Katz, S. E. Wiberley, *Inorg. Chem.* **1965**, *4*, 1157–1163.
[33] A. D. Ostrowski, S. J. Deakin, B. Azhar, T. W. Miller, N. Franco, M. M. Cherney, A. J. Lee, J. N. Burstin, J. M. Fukuto, I. L. Megson, P. C. Ford, *J. Med. Chem.* **2010**, *53*, 715.

Received: October 15, 2014
Published Online: ■

Model Complex for NO Release

Keywords: Nitric oxide / Nitroxyl / Nitrogen oxides / Ruthenium / Kinetics / Medicinal chemistry

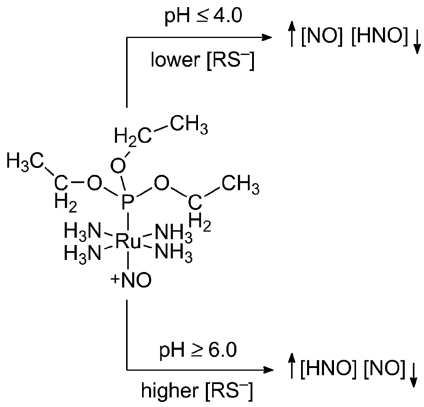

The concentration of nitric oxide and nitroxyl generated from the reaction between *trans*-[RuNO(NH$_3$)$_4$P(OEt)$_3$](PF$_6$)$_3$ and cysteine can be modulated by altering the pH. The nucleophilic attack of RS$^-$ yielded mostly *trans*-[Ru(NH$_3$)$_4$P(OEt)$_3$N(O)SR]$^{2+}$ at pH ≤ 4.0 and *trans*-[Ru(NH$_3$)$_4$P(OEt)$_3$-N(O)(SR)$_2$]$^{2+}$ at pH ≥ 6.0, which decompose into NO and HNO, respectively.

